consequence of this intermediate's ability to delocalize the unsaturation.

Acknowledgment. This work was supported by the National Science Foundation. Ruthenium used in these studies was provided on loan by Johnson Matthey, Inc.

Registry No. $Ru_3(CO)_{12}$, 15243-33-1; $Ru_3(CO)_{11}(P(OCH_3)_3)$, 82532-25-0; $Ru_3(CO)_{10}(P(OCH_3)_3)_2$, 78168-08-8; $Ru_3(CO)_9(P(OCH_3)_3)_3$, 38686-18-9; $Ru_3(CO)_{11}(P(p\text{-tolyl})_3)$, 83343-69-5; $Ru_3(CO)_{10}(P(p\text{-tolyl})_3)_2$, 100898-68-8; $Ru_3(CO)_9(P(p\text{-tolyl})_3)_3$, 38686-54-3; $Ru_3(CO)_{11}(P(o\text{-tolyl})_3)$, 86276-87-1; $Ru_3(CO)_{10}(P(o\text{-tolyl})_3)_2$, 100898-69-9; $Ru_3(CO)_9(P(o\text{-tolyl})_3)_3$, 100898-70-2; $Ru_3(CO)_{11}PPh_3$, 38686-52-1; $Ru_3(CO)_9(PPh_3)_3$, 15663-31-7; $Ru(CO)_5$, 16406-48-7; $Ru_2(CO)_6Cl_4$, 22594-69-0; $Ru(CO)_4(C_2H_4)$, 52621-15-5; $Ru(CO)_4(P(OCH_3)_3)$, 75641-93-9; $Ru(CO)_3(P(OCH_3)_3)_2$, 31541-94-3; $Ru(CO)_4PPh_3$, 21192-23-4; $Ru(CO)_3(PPh_3)_2$, 14741-36-7; THF, 109-99-9; 2-MeTHF, 96-47-9; CCl_4, 56-23-5; $P(OCH_3)_3$, 121-45-9; PPh_3, 603-35-0; $H_2C{=}CH_2$, 74-85-1; CO, 630-08-0; octane, 111-65-9; cyclohexane, 110-82-7; diglyme, 111-96-6; benzene, 71-43-2; pyridine, 110-86-1; acetonitrile, 75-05-8.

Four Zirconium Iodide Cluster Phases Centered by Boron, Aluminum, or Silicon

Jerome D. Smith and John D. Corbett*

Contribution from Ames Laboratory-DOE[1] and Department of Chemistry, Iowa State University, Ames, Iowa 50011. *Received October 4, 1985*

Abstract: Well-faceted crystals of $Zr_6I_{12}B$, $MZr_6I_{14}B$ (M = Cs or K), $Cs_{0.7}Zr_6I_{14}Al$, and $Cs_{0.3}Zr_6I_{14}Si$ are obtained in good yield from reactions of stoichiometric amounts of Zr, ZrI_4, CsI, or KI when appropriate and B, Si, or AlI_3 at 850 °C in sealed tantalum containers after 2 weeks. The compounds were established to be isostructural with $Zr_6I_{12}C$ (space group $R\bar{3}$) or $(Cs)Zr_6I_{14}C$ (*Cmca*), and one crystal structure for each of the four examples (M = Cs) was refined with use of single-crystal X-ray techniques. All of these compounds contain Zr_6I_{12}-type clusters with an interstitial B, Al, or Si (Z) atom in the center of the cluster at full occupancy. Changes in Z cause substantial changes in the host lattice, most directly in the size of the cluster where $\bar{d}$(Zr–Zr) ranges between 3.580 Å (Si) and 3.195 Å ($Zr_6I_{12}C$). The observed $\bar{d}$(Zr–Z) values are tenths of an angstrom less than those consistently observed in ZrZ_x phases, especially for aluminum. Extended-Hückel calculations illustrate the important role of the interstitial in providing both additional electrons and strong Zr–Z bonding to the cluster. Increasing Hi_i values for the interstitial valence orbitals in the order C, Si, B, Al reduce Zr–Z bonding and charge transfer to the interstitial atom, especially for aluminum 3p orbitals. The bonding in Zr_2Al shows some comparable properties.

In the past 3 years, the bonding of several light elements within metal cluster halides has been reported. The earlier examples pertained to carbon within condensed M_6X_{12}-type octahedral metal clusters of rare-earth and early transition metals where the cluster aggregation ranged from dimers through infinite chains and sheets.[2-8] Very recently, the bonding of several second-period elements—Be, B, C, N—within a variety of isolated $Zr_6Cl_{12}^{n-}$ clusters ($0 \le n \le 4$) has also been noted,[9] and the synthesis and characterization of three types of carbon-centered zirconium iodide clusters, $Zr_6I_{12}C$, $Zr_6I_{14}C$, and $MZr_6I_{14}C$ (M = K, Rb, or Cs), have been reported in detail.[10] Extended-Hückel calculations on the carbon-centered as well as on the hypothetical unoccupied iodide clusters of these types show that, as expected, the carbon 2s and carbon 2p orbitals interact strongly with molecular orbitals in the unoccupied clusters which are primarily zirconium 4d to stabilize the centered cluster via four rather low-lying Zr–C bonding orbitals. Four other Zr–Zr bonding orbitals are unchanged, so that a total of 14–16 electrons from the zirconium and carbon that remain after the iodine valence band is filled can be accommodated in these Zr–C and Zr–Zr bonding orbitals, as observed.

Zirconium iodide clusters appear to be particularly adaptable in accommodating other interstitial atoms, perhaps because of the larger halide and greater covalency of the bonding. One example occurs with the relatively large, centered potassium atom in the remarkable $Zr_6I_{14}K$.[11] Here somewhat different factors appear to be important in the bonding; the potassium 4p orbitals are now too high in energy to interact well with the apropriate Zr–Zr bonding orbitals, and interstitial bonding occurs mainly via the potassium 4s orbital. In compensation, however, additional Zr–I bonding results from improved Zr–I overlap when the zirconium octahedron expands to accommodate the larger interstitial and comes closer to the size of the cube defined by the 12 edge-bridging iodines.

These contrasting examples of interstitial bonding have led us to investigate whether other interstitial atoms might be included in the center of octahedral zirconium iodide clusters. Herein we report the synthesis, structural characterization, and the results of extended-Hückel calculations on four metal cluster halides containing three new interstitial atoms, boron in $Zr_6I_{12}B$ and $MZr_6I_{14}B$ (M = Cs or K), silicon in $Cs_{0.3}Zr_6I_{14}Si$, and aluminum in $Cs_{0.7}Zr_6I_{14}Al$.

Experimental Section

Materials. The purity, preparation, and handling of reactor grade Zr and ZrI_4 have been previously described.[12] Zirconium powder was prepared from metal strips through the formation and decompositon in

(1) Operated for the U. S. Department of Energy by Iowa State University under contract No. W-7405-Eng-82. This research was supported in part by the Office of Basic Energy Sciences, Materials Sciences Division.
(2) Warkentin, E. Masse, R.; Simon, A. *Z. Anorg. Allg. Chem.* **1982**, *491*, 323.
(3) Simon, A.; Warkentin, E. *Z. Anorg. Allg. Chem.* **1983**, *497*, 79.
(4) Schwanitz, U.; Simon, A. *Z. Naturforsch. B* **1985**, *40*, 710.
(5) Simon, A. *J. Solid State Chem.* **1985**, *57*, 2.
(6) Ford, J. E.; Corbett, J. D.; Hwu, S.-J. *Inorg. Chem.* **1983**, *22*, 2789.
(7) Hwu, S.-J.; Corbett, J. D.; Poeppelmeier, K. R. *J. Solid State Chem.* **1985**, *57*, 43.
(8) Hwu, S.-J.; Ziebarth, R. P.; Winbush, S. v.; Ford, J. E.; Corbett, J. D. *Inorg. Chem.*, accepted for publication.
(9) Ziebarth, R. P.; Corbett, J. D. *J. Am. Chem. Soc.* **1985**, *107*, 4571.
(10) Smith, J. D. Corbett, J. D. *J. Am. Chem. Soc.* **1985**, *107*, 5704.
(11) Smith, J. D.; Corbett, J. D. *J. Am. Chem. Soc.* **1984**, *106*, 4618.
(12) Guthrie, D. H.; Corbett, J. D. *J. Solid State* Chem. **1981**, *37*, 256.

0002-7863/86/1508-1927$01.50/0

vacuum of ZrH_{2-x}.[8] Reagent-grade alkali metal iodides were distilled under vacuum prior to use. National Bureau of Standards silicon (SRM-640) was used as received for the syntheses of the silicide. The aluminum source was AlI_3 which had been prepared from the elements at 200 °C and sublimed twice under vacuum before use. Both amorphous boron (Alfa, 95%, −325 mesh) and the high purity element (Research Organic/Inorganic, 5–9's) were used in syntheses. The lattice parameters of samples made from these two sources did not differ significantly, although the amorphous boron gave more nearly complete reactions, presumably because of its higher surface area.

Syntheses. All reactions were run in sealed Ta tubes with use of techniques described previously.[7,12] Well-crystallized samples of $CsZr_6I_{14}B$ and $KZr_6I_{14}B$ were obtained in >90% yields by reaction of stoichiometric quantities of Zr powder, ZrI_4, amorphous B, and CsI or KI at 850 °C for 2 weeks. The indicated yields were generally estimated both from careful powder pattern analysis and visually, the products of interest invariably appearing as well-faceted, gemlike, black crystals. A structural analysis of the cesium boron product showed the compound was stoichiometric in alkali metal content, and the same was inferred for the potassium compound based on the difference between its lattice parameters and those of $CsZr_6I_{14}B$ compared with the difference in lattice parameters between $CsZr_6I_{14}C$ and $KZr_6I_{14}C$.[10]

Well-crystallized $Zr_6I_{12}B$ was formed in high yield in the stoichiometric reaction of Zr, ZrI_4, and amorphous boron at 850 °C for 2 weeks. Efforts to prepare an "$NaZr_6I_{12}B$" phase isoelectronic with $Zr_6I_{12}C$[10] in a similar manner gave only unreacted NaI plus a high yield of black crystals that gave a powder pattern and lattice parameters therefrom that were not significantly different from those of $Zr_6I_{12}B$. An attempt at the synthesis of $Zr_6I_{14}B$ under comparable conditions produced $Zr_6I_{12}B$.

The new $Cs_{0.30}Zr_6I_{14}Si$ was first found in a reaction (850 °C, 3 days) of stoichiometric amounts of CsI, ZrI_4, and Si with a large excess of Zr strips. The remainder of the products consisted of α,β-ZrI_2,[13] $Cs_3Zr_2I_9$,[14] and ZrI_3, suggesting an incomplete reaction. Refinement of its structure showed a substantial substoichiometry in cesium, as written. Subsequent reactions that were loaded with a twofold excess of CsI and Zr powder but with stoichiometric proportions of ZrI_4 and Si and heated for 2 weeks at 850 °C resulted in a 30–40% yield of well-faceted black crystals (plus ZrI_3 and $Cs_3Zr_2I_9$) that gave lattice parameters within 3σ of those of the above $Cs_{0.3}Zr_6I_{14}Si$, indicating this cesium content is probably an upper limit.

Reactions of stoichiometric amounts of CsI, ZrI_4, AlI_3, and Zr powder at 850 °C for 2 weeks resulted in a 50% yield of black crystals and a shiny black powder plus ZrI_3, ZrI_4, and $Cs_3Zr_2I_9$. The black powder gave the same pattern and lattice constants as the crystals which were determined to be $Cs_{0.7}Zr_6I_{14}Al$ by X-ray diffraction. Reactions under comparable conditions, using stoichiometric quantities of the appropriate materials to produce $Zr_6I_{12}Z$ or $Zr_6I_{14}Z$, Z = Al or Si, were not successful.

Unsuccessful Reactions. A number of reactions were run between 600 and 850 °C, utilizing ZrI_4, Zr, ZrNI as a nitrogen source and, sometimes, CsI. These resulted only in ZrI_3, α,β-ZrI_2, ZrN_x, plus $Cs_3Zr_2I_9$ when CsI was present. Oxygen insertion attempts involved reactions of either α-$ZrO_{0.4}$ or ZrO_2 with ZrI_4, Zr, and, occasionally, CsI. These produced at best ca. 5% yield of black gemlike crystals, comparable to earlier results.[20] Those made without CsI present were invariably $Zr_6I_{12}C$, as demonstrated before,[10] while the product obtained with CsI present gave a "$CsZr_6I_{14}$" pattern with a relatively large cell ($V \sim 2950$ Å^3). Spectrographic emission analysis of the ZrO_2 utilized showed a substantial contamination by silicon, which is thought to have originated with the silica gel over which precursor $ZrOCl_2$ solutions had been passed in order to remove hafnium. The large cell for pseudoternary cesium salt is typical of the larger values found earlier[20] for this structure where adventitious interstitial impurities were evidently responsible. Spectrographic analysis of several such iodide products showed a significant silicon content (~1%) together with small but discernable amounts of boron and aluminum. Unrecognized chips of Pyrex glass in the ZrI_4 starting material are certainly a feasible source of what were probably mixed interstitial products. In any case, considerable care is needed to avoid the formation of these very stable, readily formed, and well-crystallized impurity phases.

Table I. Cell Parameters (Å) and Volumes (Å^3) of Zirconium Iodide Cluster Compounds[a]

compound	a	b	c	V
$KZr_6I_{14}B$	15.849 (2)	14.277 (2)	12.876 (1)	2913 (1)
$CsZr_6I_{14}B$	15.939 (2)	14.263 (2)	12.974 (1)	2950 (1)
$Zr_6I_{12}B$	14.534 (1)		9.986 (1)	1825 (1)
$Cs_{0.3}Zr_6I_{14}Si$	15.997 (1)	14.283 (1)	12.996 (1)	2969 (1)
$Cs_{0.7}Zr_6I_{14}Al$	15.907 (1)	14.284 (1)	12.973 (1)	2948 (1)
$K_{0.58}Zr_6I_{14}C$[b]	15.727 (2)	14.278 (3)	12.798 (2)	2874 (1)
$KZr_6I_{14}C$	15.757 (2)	14.314 (2)	12.807 (2)	2889 (1)
$CsZr_6I_{14}C$	15.803 (2)	14.305 (3)	12.934 (1)	2924 (1)
$Zr_6I_{12}C$	14.508 (1)		10.007 (1)	1822 (1)

[a] $MZr_6I_{14}X$ phases crystallize in the orthorhombic space group *Cmca* and $Zr_6I_{12}X$ in the space group $R\bar{3}$, reported here in the hexagonal setting. All values were obtained by means of Guinier powder diffraction. [b] These four sets of data are from ref 10.

X-ray Powder Diffraction. Preliminary product identification utilized X-ray powder data obtained with a focusing Guinier camera (Enraf-Nonius) equipped with a silicon monochromator to give clean Cu $K\alpha_1$ radiation. Sampling mounting has been previously described.[15] NBS silicon (SRM-640) was included as an internal standard, the five observed lines being fitted to known diffraction angles by a quadratic function in position with a least-squares program. The powder patterns were indexed with the aid of data calculated for the known structures, and the corresponding lattice constants were determined by standard least-squares refinement. Lattice constants of the new zirconium cluster phases are given in Table I together with data for other phases for reference.

Single-Crystal X-ray Studies. Reaction containers were opened in a drybox, and crystals were mounted under low magnification in thin-walled glass capillaries, typically 0.3 mm i.d. Single crystal data sets were collected on either a SYNTEX $P2_1$ diffractometer with the aid of Mo $K\alpha$ radiation (no monochromator, Zr filter to eliminate Mo $K\beta$) and $2\theta/\theta$ scans or a DATEX instrument with monochromatized Mo $K\alpha$ radiation (λ = 0.71069 Å) and ω-scans. A summary of the details of the investigations is given in Table II. An empirical absorption correction was carried out in all cases with the aid of full-circle ϕ-scan data obtained on the diffractometer. Programs used in single-crystal structural refinement have been previously referenced.[7] Molecular drawings were obtained with use of the Ortep program. Atomic scattering factors included corrections for the real and imaginary contributions to anomalous dispersion.[16]

The inclusion of a secondary extinction correction was especially important for the two boride crystals. As noted previously for the carbon-centered zirconium iodide cluster phase, large reflections make a large, positive contribution to the electron density in the center of the cluster in these two space groups. Therefore, a secondary extinction correction is necessary for the successful refinement of the interstitial atom when the data are obtained from well-formed crystals. In the present cases, inclusion of the secondary extinction correction[17] resulted in a drop in both R and R_w of a few percent and a significant increase in the magnitude of the electron density refined at the center of the cluster.

Initial positions for the heavy atoms in each refinement were taken from the isostructural carbon-centered zirconium iodide cluster.[10] Since substoichiometry at the alkali metal site has previously been observed in $K_xZr_6I_{14}C$ and in some chloride clusters,[9] the occupancy of the cesium was also allowed to vary. With $CsZr_6I_{14}B$ the result was not significantly different from unity, and so it was returned to that value and not varied further. In the final stages of refinement, all atoms were refined anisotropically except the interstitials which were refined isotropically. The aluminum in $Cs_{0.7}Zr_6I_{14}Al$ gave an isotropic B of 2.2 (2) Å^2, which compared with a range of 0.2 to 1.4 for other interstitial atoms refined in this and related studies and an average of 1.3 for the other atoms in the same refinement. On the other hand, fixed B's of 1.0 or 0.6 for the aluminum atom reduced the occupancy to only 0.93 (3) or 0.88 (3), respectively. Data from a second crystal gave no better results. The powder patterns from both ground crystals and the powdered product were sharp and yielded the same lattice constants, indicating the products were completely uniform in composition. The high (50%) yield of the product and the size and occupancy of the cavity are also inconsistent with the presence of other interstitials. In addition, except for the very unusual cluster compound $Zr_6I_{14}K_x$ (x = 0.46 and 1),[11] no fractional occupancy of the interstitial position has been observed here or in many chloride clusters. In light of all of these circumstances, the aluminum

(13) Corbett, J. D.; Guthrie, D. H. *Inorg. Chem.* **1982**, *21*, 1747.
(14) Guthrie, D. H.; Meyer, G.; Corbett, J. D. *Inorg. Chem.* **1981**, *20*, 1192.
(15) Daake, R. L.; Corbett, J. D. *Inorg. Chem.* **1978**, *17*, 1192.
(16) "International Tables for X-Ray Crystallography", Kynoch Press: Birmingham, England, 1968 and 1974; Vol. III and IV.
(17) Coppens, P.; Hamilton, W. C. *Acta Crystallogr.* **1970**, *A26*, 71.
(18) Hubbard, C. R.; Jacobson, R. J., Ames Laboratory, unpublished program, 1969.
(19) Hoffmann, R. *J. Chem. Phys.* **1963**, *39*, 1397.
(20) Guthrie, D. H.; Corbett, J. D. *Inorg. Chem.* **1982**, *21*, 3290.

Table II. Data Collection and Refinement Parameters

	$CsZr_6I_{14}B$	$Cs_{0.3}Zr_6I_{14}Si$	$Cs_{0.7}Zr_6I_{14}Al$	$Zr_6I_{12}B$
space group	*Cmca*	*Cmca*	*Cmca*	$R\bar{3}$
Z	4	4	4	3
crystal dimen,	0.25	0.15	0.28	
mm	0.18	0.12	0.18	
	0.14	0.08	0.12	
$2\theta_{max}$, deg	55	55	50	50
reflections				
measured	4026	3847	1499	1304
observed[a]	1977	1575	596	999
independent	1043	876	596	707
R_{av}, %	3.1	5.2		5.5
R^b, %	4.0	5.7	3.6	6.6
R_w^c, %	4.0	6.5	3.9	8.4
secondary extinct. coeff. (10^{-4})	0.7 (1)		0.29 (5)	4.1 (11)
absorption coeff.	180	171	177	180
μ, L/cm				
range of transm. coeff.	0.79–1.00	0.39–0.99	0.60–1.00	0.55–0.99
no. of parameters	101	101	101	46
no. of variables	55	57	57	30

[a] $F_{obsd} \geq 3\sigma_F$ and $I_{obsd} > 3\sigma_I$. [b] $R = \sum(|F_o| - |F_c|)/\sum|F_o|$. [c] $R_w = [\sum w(|F_o| - |F_c|)^2/\sum w|F_o|^2]^{1/2}$.

site is considered to be fully occupied. The other three crystals studied gave B's of 0.3 to 0.6 for the interstitial when fixed at unit occupancy.

The data sets shared a significant dependence of $\Sigma w(|F_o| - |F_c|)^2$ on F_o, and a reweighting of the data sorted on F_o in 10 to 15 overlapping groups with a statistically meaningful procedure[18] resulted in slightly lower positional standard deviations. Final electron density difference maps showed no peaks greater than corresponding to $Z = \pm 0.5$ except in $Zr_6I_{12}B$ where peaks of $Z \simeq \pm 1$ appeared in random positions. This may be related to truncation problems that were suggested by the presence of diffuse waves in the map.

Extended-Hückel Calculations. In order to understand the bonding in these interstitial clusters better, noniterative extended-Hückel calculations[19] were carried out on isolated $Zr_6I_{18}Z^{n-}$ clusters (Z = B, Al, or Si). This unit consists of the 14-electron $Zr_6I_{12}Z^{6-n}$ clusters present in the $(Cs)Zr_6I_{14}Z$ phases together with the six I^- atoms that are terminal to each metal atom in the cluster and important in the correct electronic description of the cluster.[10] The geometries and distances used were those observed in the structures of the appropriate phases except that very small changes were made to give the clusters (including iodine) D_{2h} symmetry rather than the lower crystallographic C_{2h} point symmetry. The resulting orbital energies are insignificantly different from those for the C_{2h} cluster. The Cartesian coordinates of these and the orbital parameters utilized are available as supplementary material.

Results and Discussion

This investigation was initially targeted on the cause(s) for both the variability in the lattice parameters and the residual electron densities found within the clusters in the reported "$CsZr_6I_{14}$" phase.[20] The conclusion is that interstitial atoms are present, in fact necessary, in the zirconium cluster iodides. The synthesis and characterization of the phases $Zr_6I_{14}C$, $MZr_6I_{14}C$ (M = Cs, Rb, or K), and $Zr_6I_{12}C$ containing carbon-centered $Zr_6I_{12}C$-type clusters have already been reported.[10] Here we describe four additional clusters containing three different interstitial atoms: boron in $MZr_6I_{14}B$ (M = Cs or K) and $Zr_6I_{12}B$, silicon in $Cs_{0.3}Zr_6I_{14}Si$, and aluminum in $Cs_{0.7}Zr_6I_{14}Al$. The latter two represent the first examples of third period elements occupying the centers of the transition-metal cluster halides. The new phases are obtained in good yields and as well-faceted crystals from reactions of approximately stoichiometric quantities of ZrI_4, Zr (sometimes in excess), M^II when appropriate, and B, Si, or AlI_3 at 850 °C for 1–2 weeks. Transport reactions seem evident.

Structural Results. The structures of the boron-, silicon- and aluminum-containing clusters were refined by single-crystal X-ray diffraction to give the atomic coordinates and standard deviations compiled in Table III. The anisotropic thermal parameters and the observed and calculated structure factor amplitudes for each structural solution are available as supplementary material. Table IV contains the important bond lengths in the four structures together with those for the analogous $Zr_6I_{14}C$ for comparison. The isolated cluster in $Cs_{0.3}Zr_6I_{14}Si$ is shown in Figure 1.

The phases $Zr_6I_{12}Z$ and $MZr_6I_{14}Z$ (Z = interstitial atom; M = K, Cs, or nothing) are both based on $Zr_6I_{12}Z$-type clusters in which slightly distorted octahedra of zirconium atoms with 12 inner (i) iodine atoms bridging the edges thereof are also centered by an interstitial atom Z. As with virtually all clusters and their condensation products, each zirconium is also bonded to a more distant iodine atom in a terminal or exo (a) position so that Z, Zr, and I^a are nearly colinear. The stoichiometries of the basic Zr_6I_{12} and $Zr_6I_{14}X$ structure types are then the result of the way in which the clusters are interconnected through shared iodines at terminal positions to form three-dimensional cluster networks, as has been described earlier.[10] Briefly, the six I^i (I1) atoms in

Table III. Final Atomic Positions

	x	y	z
	$Cs_{0.30(1)}Zr_6I_{14}Si$		
I1	0.12550 (8)	0.08897 (8)	0.2475 (1)
I2	0.12583 (7)	0.2539 (1)	0.0069 (1)
I3	1/4	0.3437 (1)	1/4
I4	0	0.1589 (1)	0.7647 (2)
I5	0.2468 (1)	0	0
Cs[a]	0	0	0
Zr1	0.3865 (1)	0.0691 (2)	0.8853 (2)
Zr2	0	0.3545 (2)	0.8932 (2)
Si	1/2	1/2	1/2
	$Cs_{0.69(1)}Zr_6I_{14}Al$		
I1	0.1251 (1)	0.08941 (8)	0.2494 (1)
I2	0.1256 (10)	0.2560 (1)	0.0064 (1)
I3	1/4	0.3469 (2)	1/4
I4	0	0.1587 (2)	0.7624 (2)
I5	0.2472 (2)	0	0
Cs[b]	0	0	0
Zr1	0.3911 (2)	0.0662 (2)	0.8891 (2)
Zr2	0	0.3623 (3)	0.8987 (3)
Al[c]	1/2	1/2	1/2
	$CsZr_6I_{14}B$		
I1	0.035525 (4)	0.10257 (4)	0.33250 (6)
I2	0.12642 (4)	0.17766 (4)	0.32488 (6)
I3	1/4	0.34703 (8)	1/4
I4	0	0.16036 (8)	0.76037 (9)
I5	0.24802 (7)	0	0
Cs[d]	0	0	0
Zr1	0.39291 (7)	0.06556 (8)	0.89102 (9)
Zr2	0	0.3637 (1)	0.9002 (1)
B	1/2	1/2	1/2
	$Zr_6I_{12}B$		
I1	0.035493 (7)	0.10245 (6)	0.33197 (8)
I2	0.12708 (6)	0.17821 (7)	0.3270 (1)
Zr	0.14634 (9)	0.04146 (9)	0.1346 (1)
B	0	0	0

[a] Occupancy refined to 0.30 (1). [b] Occupancy refined to 0.69 (1). [c] Occupancy of 0.93 (3) for $B = 1.0$; 1.0 for $B = 2.2$ (2), see text. [d] Unit occupancy.

Table IV. Bond Distances in Interstitial-Centered Zirconium Iodide Clusters[a]

		$Zr_6I_{14}C$[b]	$CsZr_6I_{14}B$	$Cs_{0.3}Zr_6I_{14}Si$	$Cs_{0.7}Zr_6I_{14}Al$		$Zr_6I_{12}B$
Zr–Zr intralayer[c]							
Zr1–Zr1	(×2)	3.355 (3)	3.414 (2)	3.632 (4)	3.462 (5)	(×6)	3.291 (2)
Zr1–Zr2	(×4)	3.284 (2)	3.349 (2)	3.562 (3)	3.408 (4)		
Zr–Zr interlayer							
Zr1–Zr1	(×2)	3.345 (3)	3.390 (2)	3.574 (4)	3.444 (5)	(×6)	3.292 (2)
Zr1–Zr2	(×4)	3.292 (2)	3.357 (2)	3.574 (3)	3.391 (4)		
Zr1–Zr1	(×2)	4.738 (3)	4.811 (2)	5.096 (4)	4.833 (5)	(×3)	4.655 (3)
Zr2–Zr2	(×1)	4.560 (4)	4.671 (3)	4.996 (6)	4.730 (8)		
Zr–I^i							
Zr1–I5	(×2)	2.847 (2)	2.865 (1)	2.861 (3)	2.866 (4)	(×6)	2.877 (2)
Zr1–I1	(×2)	2.860 (2)	2.886 (1)	2.887 (2)	2.880 (3)	(×6)	2.869 (2)[d]
Zr1–I2	(×2)	2.868 (2)	2.895 (1)	2.898 (3)	2.891 (3)		
Zr2–I1	(×2)	2.840 (2)	2.840 (2)	2.875 (2)	2.862 (4)		
Zr2–I2	(×2)	2.848 (2)	2.876 (1)	2.881 (2)	2.872 (3)		
Zr–I^{i-a}							
Zr1–I4	(×2)	2.908 (2)	2.933 (1)	2.957 (3)	2.932 (3)	(×6)	2.951 (2)[d]
						(×6)	2.919 (1)
Zr–I^{a-i}							
Zr2–I4	(×2)	3.491 (3)	3.421 (1)	3.256 (4)	3.405 (5)	(×6)	3.344 (2)[d]
Zr–I^{a-a}							
Zr1–I3	(×4)	3.138 (2)	3.177 (1)	3.068 (2)	3.137 (3)		
Zr–interstitial							
Zr1–int.	(×4)	2.369 (2)	2.406 (1)	2.548 (2)	2.442 (3)	(×6)	2.327 (1)
Zr2–int.	(×2)	2.280 (1)	2.335 (2)	2.498 (3)	2.356 (4)		
M–I							
M–I1	(×4)		4.011 (1)	3.998 (1)	4.007 (2)		
M–I2	(×4)		4.163 (1)	4.149 (1)	4.168 (2)		
M–I4	(×2)		3.860 (1)	3.808 (2)	3.826 (3)		
M–I5	(×2)		3.953 (1)	3.948 (2)	3.932 (3)		

[a] Superscript i and a on iodine atoms refer to inner edge-bridging and outer terminal functions on the zirconium cluster, respectively. [b] Data from ref 10. [c] Referred to approximately close-packed layers that run roughly horizontally and perpendicular to the page in Figure 1.[10] [d] In Zr_6I_{12} the Zr–I^i distances are all Zr1–I2 while the Zr–I^{i-a} and Zr–I^{a-i} distances are both Zr1–I1.

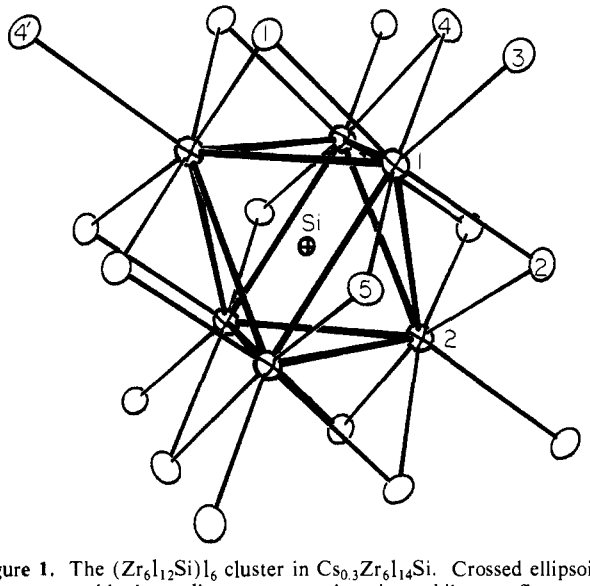

Figure 1. The $(Zr_6I_{12}Si)I_6$ cluster in $Cs_{0.3}Zr_6I_{14}Si$. Crossed ellipsoids interconnected by heavy lines represent zirconium while open figures are iodine. A twofold axis through atoms I5 and Si and a mirror plane containing I4, Si, and Zr2 give the cluster C_{2h} symmetry with an inversion center at Si. (I1, I2, I5 = I^i, I3 = I^{a-a}; I4 = I^{i-a}; I4′ = I^{a-i}; 50% probability ellipsoids.)

$Zr_6I_{12}X$ that bridge the edges around the waist of the cluster normal to its $\bar{3}$ axis are three-coordinate because they also serve as more distant I^a to adjacent clusters, i.e., I^{i-a}. The interconnectivity of the $(M)Zr_6I_{14}Z$ phase is more complex since only two of the six terminal iodines of each cluster are shared, as above, the four remaining iodines being two-coordinate outer atoms that only bridge between clusters The formulation of the Zr_6I_{12} matrix is then $Zr_6I^i{}_6I^{i-a}{}_{6/2}I^{a-i}{}_{6/2}$ and that of Zr_6I_{14} is $Zr_6I^i{}_{10}I^{i-a}{}_{2/2}I^{a-i}{}_{2/2}I^{a-a}{}_{4/2}$. The M^1 atom in the latter, if any, occupies a 12-coordinate position within nominally close-packed layers of iodine (and Z) atoms. This site is unoccupied in $Zr_6I_{14}(C,B)$ and in the long-known and isostructural $(Nb,Ta)_6X_{14}$ phases[21,22] which, of course, lack the interstitial atom Z.

Because of the counter disposition of terminal halogen and interstitial Z atoms, they are in effect in competition for radially directed orbitals on the metal. The tetragonal compression of the metal octahedron in the M_6X_{14} phases has been shown[10] to be a direct result of the asymmetric bonding of halogen at the terminal positions and its effect on bonding within the cluster. The greater distances of all of the three-coordinate terminal atoms in the $Zr_6X_{12}Z$ phases similarly result in markedly smaller metal–metal distances so that clusters in the two structure types are not easily intercompared.

Average distances of various types in the new clusters are given in Table V along with those in $Zr_6Cl_{14}C$ for comparison. The cluster sizes are naturally a reflection of the effective size and bonding of the interstitial, but these are also influenced, as above, through secondary changes in terminal iodine distances. Matrix effects are also thought to be important, I^i–I^i contact repulsions in particular that restrict the contraction of the metal cluster, and result in diminished Zr–I bonding, both inner and outer.

Changes in Zr–Zr, Zr–Z, and Zr–I^a bond lengths in the $(M)Zr_6I_{14}Z$ phases as well as the relatively constant Zr–I^i distances can be understood to a first approximation from simple geometry by assuming that the iodine positions remain essentially fixed by contact repulsions while the zirconium octahedra vary to accommodate the interstitial atoms. This means that the changes in Zr–Z distances and Zr–I^a distances in two different clusters should

(21) Simon, A.; von Schnering, H.-G.; Wöhrle, H.; Schäfer, H. *Z. Anorg. Allg. Chem.* **1965**, *339*, 155.
(22) Bauer, D.; von Schnering, H.-G.; Schäfer, H. *J. Less-Common Met.* **1965**, *8*, 388.

Table V. Average Bond Distances in $(M_x)Zr_6I_{14}Z$ Cluster Phases (Å)

	$Zr_6I_{14}C^a$ (14)[c]	$CsZr_6I_{14}B$ (14)[c]	$Cs_{0.3}Zr_6I_{14}Si$ (14.3)[c]	$Cs_{0.7}Zr_6I_{14}Al$ (13.7)[c]	$Zr_6I_{12}B$ (15)[c]
Zr–Zr	3.309 (3)	3.366 (3)	3.580 (3)	3.417 (4)	3.292 (2)
Zr–I^i	2.862 (2)	2.889 (1)	2.893 (2)	2.884 (3)	2.904 (2)
Zr–I^{a-i}	3.491 (3)	3.421 (1)	3.256 (4)	3.405 (5)	3.344 (2)
Zr–I^{a-a}	3.138 (2)	3.177 (1)	3.068 (2)	3.137 (3)	
Zr–Z	2.339 (2)	2.382 (1)	2.531 (2)	2.416 (3)	2.327 (1)
r_Z[b]	1.48	1.52	1.67	1.56	1.47

[a] Reference 10. [b] Effective crystal radius of the interstitial; see the text. [c] Cluster e's.

be equal in magnitude and opposite in sign, i.e., d(Z–I^a) should be constant. Furthermore, the ratio of the changes in Zr–Zr distances to Zr–Z distances in an octahedron should ideally be $1:\sqrt{2}$. At the same time the Zr–I^i distances should change by the product of Δd(Zr–Z) and the average of $^1/_2$ sin (I^i–Zr–I^i), this angle being for I^i's that are trans across the approximately square plane of inner iodines bonded to the zirconium atom (Figure 1). Since these angles are between 155 and 170°, the Zr–I^i distances should change only slightly.

Applying this model to the two extremes, $Zr_6I_{14}C$ and $Cs_{0.3}Zr_6I_{14}Si$, the difference in average Zr–Zr distances in fact yields the observed difference in the Zr–Z distances of $0.271/\sqrt{2}$ = 0.192 Å. The difference found in the complementary Zr–I^{a-i} distances is –0.235 Å, very nearly what is expected, while the Zr–I^i distances vary by only 0.03 Å. The effect that the inclusion of a silicon atom has on the geometry of the cluster is substantial indeed, and in terms of the layered nature of these structures, the zirconium atoms are now much closer to the "ideal" octahedral coordination by halogen. The Zr–Zr edges of the octahedron average 3.580 (3) Å and must be considered to represent fairly weak interactions.

The only bond distances that do not follow this argument are those for Zr–I^{a-a}, which ae only 0.07 Å shorter in $Cs_{0.3}Zr_6I_{14}Si$ than in $Zr_6I_{14}C$ even though d(Zr–Z) has increased by 0.19 Å. In fact, the Zr–I^{a-a} distances only range from 3.068 (2) to 3.195 (1) Å in all zirconium iodide phases, compared with 2.86–2.89 Å for d(Zr–I^i), 2.92 Å for the sum of crystal radii,[23] and 3.26–3,52 Å for the obviously weaker and more variable Zr–I^{a-i} where inner iodine atoms in other clusters are involved. A possible rationalization for the smaller changes of Zr–I^{a-a} bond distances compared with those for Zr–I^{a-i} is that the former may represent nearly normal Zr–I distances for this type of secondary bond to terminal atoms and that outward motion of these iodine positions simply matches any expansion of the zirconium octahedron. This is particularly reflected in variations in the *a* and *c* lattice constants (Table I) since Zr–I^{a-a} bridging between clusters is distributed mainly in these directions.

Other comparisions of distances in clusters occupied by different interstitials fare equally well. Of course, the effects of the additional alkali metal atom (and the structural change for $Zr_6I_{12}C$) perturb the geometry more, and some simple arguments do not apply. The model does serve very well to explain why the cell volumes of the $Zr_6I_{14}Z$ phases vary by only 4% (even when the effect of the addition of the alkali metal atom on cell volume is ignored) while at the same time the Zr–Zr distances change by 9%, emphasizing the need for X-ray structural studies.

Interstitial Atom Size. The effective sizes of the interstitial atoms in these clusters provide some interesing, useful, and somewhat unusual features relative to both expectation and the character of these same Zr–interstitial interactions in other compounds. The observed Zr–interstitial distances in the iodide clusters are plotted in Figure 2 according to group and structure type.

By substracting the six-coordinate crystal radius for Zr^{4+} (0.86 Å[23]) from the Zr–C distance in $Zr_6Cl_{14}C$, one obtains an effective crystal radius for the interstitial carbon, 1.48 Å (Table V). A radius of 1.46 Å is likewise obtained for $CsZr_6I_{14}C$ and $K_{0.6}Zr_6I_{14}C$,[10] and similar values apply to a variety of $Zr_6Cl_{12}C$-type clusters.[24] Furthermore, these effective radii match very well

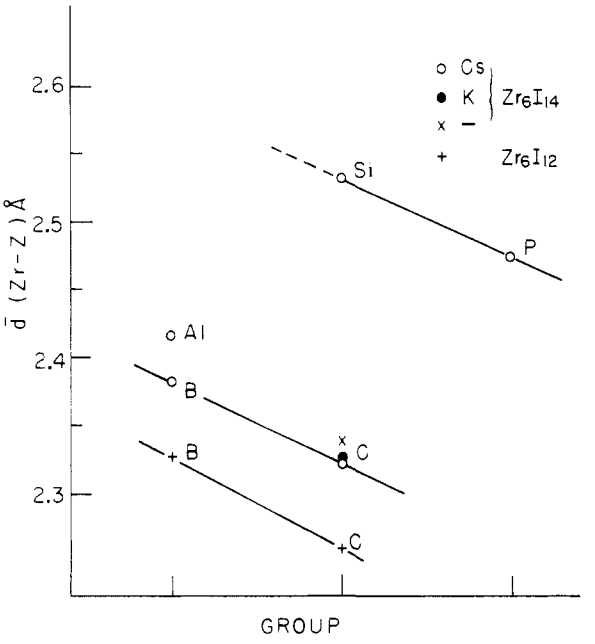

Figure 2. The average Zr–interstitial distances in clusters. $M_xZr_6I_{14}Z$: (O) Cs, (●) K, (×) nothing, $Zr_6I_{12}Z$: +. Other data from ref 10 and 31.

an average value of 1.46 Å that can be similarly deduced from a number of NaCl-type, transition-metal carbides,[25] indicating there is some transferability of these measures. Only in the $Zr_6I_{12}C$ structure does one find a smaller apparent carbon radius, 1.40 Å, along with a significantly smaller average d(Zr–Zr), 3.195 (1) Å. As discussed before, this evidently results from significant reduction in the amount of Zr–I^a bonding in a structure that has only I^{a-i} cluster connectivity and the corresponding increase in Zr–Zr and Zr–C bonding.[10] (This would not occur in a NaCl-like arrangement.) The average Zr–B distance in $CsZr_6I_{14}B$, 2.382 (1) Å, is similarly 0.06 Å larger than that in $Zr_6I_{12}B$.

Comparison of the other metal–interstitial distances produces some unusual results. First, it is difficult to make meaningful comparisons of the Zr–B distance in $CsZr_6I_{14}B$ with those in other zirconium borides because of uncertainties introduced by extensive B–B bonding and possible matrix effects in the latter; for example, the Zr–B separation in ZrB_2 (AlB_2 Type, CN (Zr) = 12), 2.54 Å, is significantly (0.16 Å) larger than in the cluster. On the other hand, the observed Zr–Si and Zr–Al distances in the $Zr_6I_{12}Z$-type clusters do clearly appear to be anomalous, presumably because this structure provides a significantly different bonding (electronic) environment from those found in the corresponding binary Zr–Si and Zr–Al phases. Thus, the Zr–Si distance in the cluster, 2.531 (2) Å, is appreciably less than either the Zr–Si distances in several binary phases or what would be expected relative to carbon based on an ~0.4 Å difference in their covalent radii. A range of 2.71–2.88 Å encompasses the shorter observed Zr–Si distances in ZrSi (CN (Zr) = 4),[26] Zr_2Si (4),[27] $ZrSi_2$ (10),[28] and CuZrSi

(23) Shannon, R. D. *Acta. Crystallogr. Sect. A* **1976**, *A32*, 751.

(24) Ziebarth, R. P.; Hwu, S.-J.; Corbett, J. D. *J. Am. Chem. Soc.*, accepted for publication.
(25) Corbett, J. D., unpublished research.
(26) Karpinskii, O. G.; Evseev, B. A. *Inorg. Mat.* **1965**, *1*, 312.

(5),[29,30] values that are 0.18–0.35 Å larger than that found in the cluster. It should be noted that a coordination number difference for zirconium is not a workable explanation. We also observe that the Zr–P distance of 2.473 Å in the recently prepared $Cs_{0.6}Zr_6I_{14}P$[31] falls short of the 2.64-Å value in ZrP (NaCl and TiP types[32]) by a similar amount.

The most striking contrast in Zr–Zr distances between the centered clusters and comparable intermetallic phases is found with aluminum. Here the observed Zr–Al distance in the cluster, 2.416 (3) Å, is *0.37 to 0.56 Å less* than the 2.84–3.03-Å range that describes Zr–Al distances in many binary intermetallics, e.g., Zr_2Al (CN (Zr) = 5),[33] Zr_4Al_3 (6),[34] ZrAl (7),[35] and Zr_2Al_3 (8).[36] Again, a significant part of this effect does not seem attributable to coordination number differences. Some evidence regarding this unusual result is provided by some relatively simple theoretical calculations, as follows.

Cluster Bonding. The bonding in centered $Zr_6I_{12}Z$-type clusters, Z = B, Al, or Si, has been investigated to gain an understanding of the role of the nonmetal in determining cluster geometry and, insofar as possible, stability. The cluster geometry used is that of the observed $Cs_xZr_6I_{14}Z$ structures with four more terminal iodine atoms at appropriate distances to fulfill the important I^{a-i} atom role, viz., $Zr_6I_{18}^{n-}$.

Figure 2 illustrates the results of bonding silicon within a slightly idealized D_{2h} zirconium iodide cluster. The hypothetical unoccupied $Zr_6I_{18}^{4-}$ cluster of the proper size on the left contains eight molecular orbitals between −10 and −7.4 eV that are primarily zirconium 4d in origin and metal–metal bonding. These MO's are drawn and labeled according to their transformation properties in O_h point group, $a_{1g}(z^2)$, $t_{2g}(xz,yz)$, $t_{1u}(xz,yz)$, and $a_{2u}(xy)$. Also relevant in this large a cluster is the slightly antibonding $e_u(xy)$. In each case, the parenthetical items identify their principal parentage in terms of d orbitals on zirconium with d_{z^2} radially directed.[10] The energies corresponding to a cluster with the observed geometry ($C_{2h} \simeq D_{2h}$) differ from those shown by insignificant amounts. Insertion of silicon without a change in cluster size produces strong interactins of its valence s and p orbitals at −17.3 and −9.2 eV, respectively, with the $a_{1g}(z^2)$ and $t_{1u}(xz,yz)$ cluster bonding orbitals to give principally the four Zr–Si bonding orbitals at lower energies, as shown. (As with carbon, a smaller amount of the interstitial p oribitals are also found in a second $t_{1u}(z^2)$ orbital that is principally Zr–I^a bonding.) The unperturbed t_{2g}^6 is the HOMO for a 14-electron cluster.

The most important changes that arise when different interstitials occupy the cluster center originate largely with changes in the AO valence energies (H_{ii} values) of the interstitial elements although smaller differences originating with cluster size and overlap are obviously also involved. Thus, the results for silicon appear appreciably different from those found with carbon where the interstitial-bonding a_{1g} and t_{1u} orbitals both lie below the relatively fixed iodine 5p and 5s bands, and these changes continue with boron and aluminum. The general differences can be best illustrated by focusing on the energies of the interstitial-bonding a_{1g} and t_{1u} levels in each relative to those of the Zr–Zr bonding t_{2g} and a_{2u} levels for the series of $Zr_6I_{18}Z^{n-}$ compounds with the observed dimensions, as shown in Figure 4. The MO energies increase markedly in response to the increasing atomic H_{ii} values for (electropositive character of) the interstitial, viz., in the order C, Si, B, Al, and as these valence energies increase, the interstitial

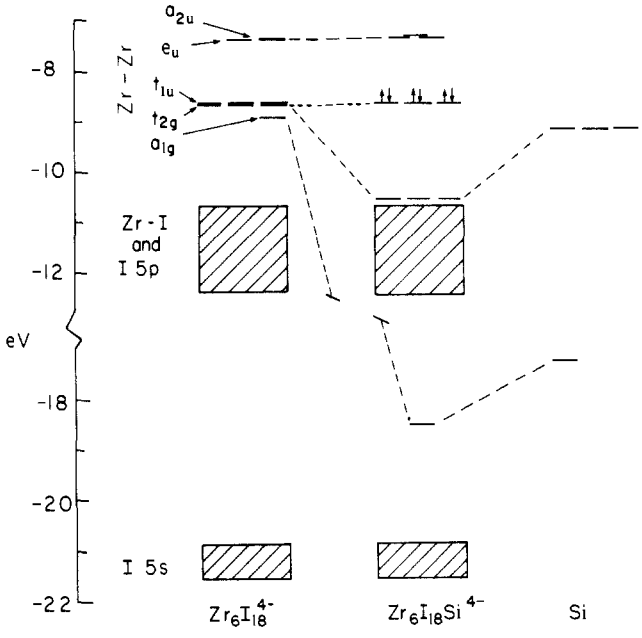

Figure 3. Molecular orbital diagrams from extended-Hückel calculations (D_{4h} symmetry). Left: $Zr_6I_{18}^{4-}$, idealized. Right: atomic Si. Center: $Zr_6I_{18}Si^{4-}$. Orbital labels refer to O_h symmetry representations. The HOMO of $Zr_6I_{18}Si^{4-}$ is the t_{2g}^6 set.

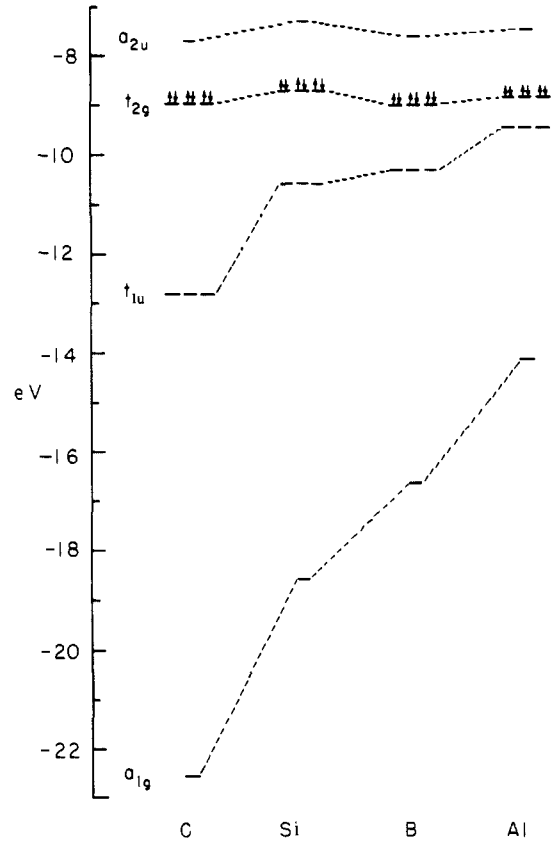

Figure 4. The energies of the interstitial-bonding a_{1g} and t_{1u} and the zirconium-bonding t_{2g} and a_{2u} molecular orbitals in $(Zr_6I_{12}Z)I_6^{n-}$ for a series of interstitial atoms. Each result pertains to the observed cluster dimensions and 14 cluster electrons.

contribution to these four bonding orbitals decreases and the zirconium contribution thereto increases.[37] A general decrease

(27) Pietrokowsky, P. *Acta Crystallogr.* **1954**, *7*, 35.
(28) Vaughan, P. A.; Bracuti, A. cited in *Struct. Rep.* **1955**, *19*, 285.
(29) Sprenger, H. *J. Less-Common Met.* **1974**, *34*, 39.
(30) The range of Zr–Si distances is also quite consistent with the observed separations in calcium–silicon and yttrium–silicon alloys when the latter are corrected according to the differences in the crystal radii of the metallic components.
(31) Rosenthal, G. L.; Corbett, J. D., unpublished research.
(32) Schönberg, N. *Acta Chem. Scand.* **1954**, *8*, 226.
(33) Wilson, C. G.; Sams, D. *Acta Crystallogr.* **1961**, *14*, 71.
(34) Wilson, C. G.; Thomas, D. K.; Spooner, F. J. *Acta Crystallogr.* **1960**, *13*, 56.
(35) Spooner, F. J.; Wilson, C. G. *Acta Crystallogr.* **1962**, *15*, 621.
(36) Renouf, T. J.; Beevers, C. A. *Acta Crystallogr.* **1961**, *14*, 469.

(37) The partial occupancy of the Zr–Zr bonding a_{2u} orbital (or the e_u alternative) in $Cs_{0.3}Zr_6I_{14}Si$ is neglected. Addition of the alkali metal and one more electron to $Zr_6I_{14}C$ causes a contraction of $\bar{d}$(Zr–Zr) by about 0.02 Å, but partial vs. full occupancy seems to have little effect on this judging from the results for $M_xZr_6I_{14}C$ where M_x = $K_{0.6}$ or $Cs_{1.0}$ (Figure 2).

Table VI. Selected Details from Extended Hückel Calculations of 14-Electron Clusters

	charge on interstitial	av Zr–Zr dist, Å	p pop (t_{1u})[c]	s pop (a_{1g})[d]	Zr–Zr reduced overlap pop[a]
$Zr_6I_{14}C$	−1.8	3.309	1.24	1.52	0.128
$CsZr_6I_{14}B$	−1.2	3.366	0.85	1.39	0.144
$Cs_{0.3}Zr_6I_{14}Si$	−0.6	3.580	0.81	1.46	0.107
$Cs_{0.7}Zr_6I_{14}Al$	+0.1	3.417	0.53	1.14	0.163
$Zr_6I_{14}K$[b]	+0.3	3.448	0.06	0.11	0.174

[a] The average overlap of atomic orbitals on adjacent zirconium atoms summed over all occupied molecular orbitals. [b] 11 cluster electrons, ref 11. [c] Occupation of interstitial p orbital in Zr–interstitial t_{1u}. [d] Occupation of interstitial s orbital in Zr–interstitial a_{1g}.

in mixing of orbitals from all three types of atoms is also evident, including the disappearance of the interstitial–$t_{1u}(z^2)$ combination noted above.

Some results of this change in interstitial atom on the bonding are quantified in Table VI. Since the energies of the valence s orbitals of carbon, boron, and silicon are considerably lower (more negative) than that of the zirconium a_{1g} orbital in the empty cluster (ca. −9 to −10 eV), the resulting a_{1g} molecular orbital is primarily interstitial in character. The degree of interstitial character of this molecular orbital can be assessed more quantitatively in terms of the orbital populations. These show that the a_{1g} molecular orbitals can be approximated as between 70 and 76% interstitial s in character for $Zr_6I_{14}C$, $CsZr_6I_{14}B$, and $Cs_{0.3}Zr_6I_{14}Si$. Similarly, the valence p orbitals of carbon, boron, and silicon lie at −11.4, −8.5, and −9.2 eV, respectively, roughly equal to that of the t_{1u} set with which they interact (−8.5 to −9 eV), and the extended-Hückel calculations show that the resulting t_{1u} set has about 61, 42, and 41% interstitial p character, respectively, in the same three compounds. The high degree of interstitial character in the four zirconium–interstitial bonding orbitals yields calculated charges on carbon, boron, and silicon of −1.8, −1.2, and −0.6, respectively, although these are probably somewhat exaggerated.

In contrast, the contribution of aluminum to the bonding in $Cs_{0.7}Zr_6I_{14}Al$ is considerably less, largely because the 3s and 3p valence orbitals now lie at −12.3 and −6.5 eV, respectively. Because the aluminum 3s orbital has about the same energy as the Zr–Zr a_{1g} orbital, the resulting Zr–Al orbital is only 57% aluminum s in character. More importantly, the contrasting energy difference between the aluminum p orbitals and the Zr–Zr $t_{1u}(xz,yz)$ set results in only a 27% contribution of that aluminum orbital to the MO, and the charge of the aluminum atom is estimated to be slightly positive, +0.1. This appears to be a fundamental result of this particular combination of atoms and not because of the small size of the cluster since virtually the same energies and interstitial charge are obtained when aluminum is centered in a silicon-sized cluster. Thus, we conclude that the lower mixing of aluminum orbitals, p especially, with the cluster and the resulting small charge transfer thereto are evidently responsible for the abnormally small $\bar{d}$(Zr–Al) value observed relative to those effective for more negatively charged interstitial atoms in the cluster (Figure 2). To the degree that this is true, the crystal radius that is found for the aluminum in this cluster may be more appropriate for the Al^+ ion than a negative charged aluminide. This aluminum-containing cluster may then be viewed as simply an intermediate stage on the way to the unusual $Zr_6I_{14}K$ where the Zr–K separation is described quite well by the sum of six-coordinate crystal radii for the cations.[11]

The apparent novelty of aluminum in this cluster persists when distances in Zr_xAl_y binary phases are used as reference, but the bonding differences are in accord with observation. The fact that the Zr–Al distances in $Cs_{0.7}Zr_6I_{14}Al$ average ~0.4 Å less than in the binaries appears to reflect a particular sensitivity of the charge transfer to aluminum on electron density or the effective zirconium oxidation state in the phase. The large number of iodine atoms present in the cluster effectively remove a good fraction of the valence electrons of zirconium. This places the oxidation state of zirconium somewhere between about 3+ and 2+ depending on whether aluminum is assigned the (unreasonable and unrealistic) limits of −5 or +3. On the other hand, a naturally higher electronic concentration in the phase Zr_2Al leads to greater occupation of what are only nonbonding (or antibonding) aluminum p states according to recent KKR-type calculations.[38] Strong Al s–Zr d interactions and over 90% of the occupied s-like states on aluminum occur in a separate valence band at ca. −4.6 eV. In contrast, strong Zr–Zr but little Zr–Al bonding is found in the conduction band at −3.3–0 eV along with 84% of the 1.3 p-like aluminum states that are occupied. It seems quite plausible that oxidaton of this system by iodine to form the cluster phase would then first empty aluminum p states to a considerable degree, leading to less screening and a markedly small size.

The quantification of these clusters that is provided by the extended-Hückel calculations also reveals some interesting features concerning the degree to which Zr–interstitial bonding dominates the geometry of these clusters. Table VI also contains values of the average Zr–Zr reduced overlap population per octahedral edge for five of the centered clusters standarized to 14 electrons. These populations are affected primarily by three factors and decrease with (a) increasing Zr–Zr distances, (b) increasing nonmetal contribution to the a_{1g} and t_{1u} bonding orbitals, and (c) increasing interactions of the remaining Zr–Zr bonding orbitals with terminal iodides. As seen in the table, the cluster with the least Zr–Zr bonding is $Cs_{0.3}Zr_6I_{14}Si$. This is not unreasonable considering the large Zr–Zr distances, the fairly short Zr–I^a distances, and the magnitude of the energy changes associated with Zr–Si bonding (Figure 3). A relatively low Zr–Zr overlap population for the $Zr_6I_{14}C$ cluster might also be expected because of the high carbon contribution to the Zr–C bonding orbitals. While the Zr–Zr bond lengths are somewhat greater in $CsZr_6I_{14}B$ than in the isoelectronic $Zr_6I_{14}C$, the lower boron contribution to the Zr–Z orbitals results in a slightly greater Zr–Zr overlap population than in $Zr_6I_{14}C$. Of the centered clusters studied, the one with the greatest amount of Zr–Zr bonding remaining is, surprisingly, $Cs_{0.7}Zr_6I_{14}Al$ with a population of 0.163, but this is a logical reflection of both the low Zr–Al bonding and the small effective interstitial size. It will be noted that this population is greater than in $Zr_6I_{14}C$, 0.128, even though the Zr–Zr distances are 0.11 Å larger, clearly a reflection of the differences in the effect of carbon and aluminum on cluster bonding.

To give some perspective of the degree to which Zr–Zr bonding is lost in favor of Zr–interstitial bonding, the averge Zr–Zr reduced overlap population of the hypothetical 14-electron empty cluster $Zr_6I_{18}^{4-}$ with Zr–Zr bond distances equal to those in $Zr_6I_{14}C$ is 0.311, compared with only 0.128 in the carbide. Even in the smaller 16-electron cluster $Zr_6I_{12}C$, the Zr–Zr reduced overlap population is only 0.166, again indicating the extent to which Zr–Zr bonding is lost. Although this comparison employs a somewhat arbitrary standard, it is clear that Zr–Zr bonding in centered clusters is of secondary importance when the s and p valence orbitals of the interstitial atoms lie at energies conducive to strong Zr–interstitial interactions. It is also important to remember that some of this Zr–Zr overlap population comes from *within* the largely interstitial-bonding t_{1u} and a_{1g} orbitals, leaving even less to attribute to the higher lying HOMO t_{2g}^6. The same is found in the "carbon band" in Zr_2Cl_2C, which can be viewed as the result of a two-dimensional condensation of $Zr_6Cl_{12}C$-type clusters.[24]

The model of bonding that emerges from these calculations is rather different than what has been presented earlier and, especially, the impression gained from the Ortep drawings of the sort shown in Figure 1. Instead of these clusters being stabilizd by very strong Zr–Zr bonds, the dominant bonding seems to originate with Zr–interstitial (and Zr–I) interactions that are augmented by weaker Zr–Zr bonding. Figure 4 shows a similar view of a cluster but with the "bonds" drawn to conform more closely to

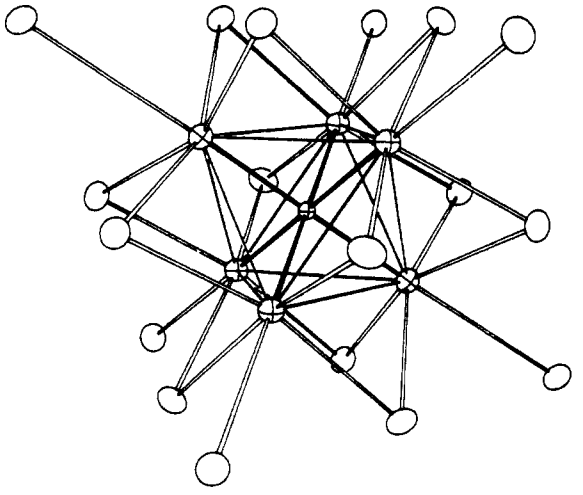

Figure 5. An Ortep drawing of a $Zr_6I_{18}Z^{n-}$ cluster that more accurately reflects the strong zirconium–interstitial bonding relative to Figure 1. Iodine: open ellipsoids. Zirconium: larger crossed ellipsoids. Interstitial: small crossed ellipsoid.

this interstitially dominated model.

Other Interstitial Atoms. Inspection of tables of H_{ii} values shows that most of the posttransition elements in the boron, carbon, and nitrogen groups have s and p orbital energies in a range suitable for good cluster–interstitial bonding, but many as yet remain untried. Oxygen and nitrogen have been attempted many times without success. While the energies of their 2s and 2p orbitals appear appropriate, the probable radii of these atoms may be so small that the Zr–I interactions could be reduced by the matrix effect (I–I repulsion) to the point that the compounds are not stable. Otherwise, the zirconium iodide clusters seem remarkably tolerant of a wide range of interstitial sizes. It is interesting to note that nitrogen-centered clusters are known for the zirconium chloride and scandium chloride systems[9,39,40] (as are clusters that contain carbon, boron, and beryllium) where the matrix effect from the halide should be much less.

Probable electronic effects must also be recognized. Presuming the phases would adopt known structures, $Zr_6I_{14}Z$ compounds with oxygen and nitrogen would contain 15 and 16 cluster-based electrons, respectively, while the apparently more stable (or more easily accessible) $M^1Zr_6I_{14}Z$ derivatives would have counts that are still one higher. Fifteen-electron iodide examples have been found several times, in $CsZr_6I_{14}C$, for example, although other analogues come up short of this through substoichiometry at the M^1 position, while sixteen in a zirconium cluster is known only for the tightly bound $Zr_6I_{12}C$. Chlorides have to date been obtained up to an electron count of fifteen and then only rarely.[9] The a_{2u} HOMO for these clusters is Zr–Zr bonding but Zr–X antibonding. Accordingly, nitrogen would be the more likely and probably only in $Zr_6I_{14}N$ or an analogue of $Zr_6Cl_{15}N$ while oxygen seems unlikely on both an electronic and a size basis. In addition, zirconium metal provides a very good alternative sink for oxygen or nitrogen through formation of the α-phase ZrO_x or ZrN_y, $x \leq 0.4$ and $y \leq 0.3$. So far no $(Nb,Ta)_6X_{12}$-type clusters have been synthesized with more than 16 electrons. Although the calculated HOMO–LUMO gap at that point is small in the clusters studied here, about 0.5 eV with carbon and much less with larger interstitials (Figure 3), the additional orbital necessary is somewhat antibonding. In addition, important questions of alternate phase stability are not addressed in such a consideration.

Attempts to include the larger silicon and aluminum atoms in the center of zirconium chloride clusters have thus far been unsuccessful,[39] again perhaps because of dominant Zr–interstitial requirements that produce unfavorable Zr–Cl bonding. There is one reported nitrogen-centered cluster in the lanthanide halide systems, Gd_2Cl_3N,[41] but here the nitrogen is located in a smaller and very distorted tetrahedral cluster. Similar size arguments can be invoked to account for the occurrence of dimeric carbon units instead of isolated carbon atoms in the much larger octahedral clusters of some of the lanthanide halides.[2,42]

Finally, we must note the existence of a large number of organometallic metal–metal bonded clusters that contain somewhat comparable centered heteroatoms (e.g., ref 43 and 44), but nearly all of these are composed of appreciably more electron-rich transition metals. In contrast, at the time of a 1980 review[45] only one octahedral cluster was known for a titanium family element, a cyclopentadienyl titanium oxide (together with one zirconium chloride omission[46]). The considerable number of zirconium, scandium, and lanthanide halide examples that have been found since then, and with every bit as large a variety of interstitial atoms at least for zirconium, clearly depend on somewhat different electronic requirements. Clusters of the latter metals involve only $d^{1.5}$ to d^2 states, and the electron shortage and weak bonding are augmented by both additional electrons from the interstitial atom and, especially, strong metal–interstitial bonding.

Acknowledgment. The authors express their appreciation to Dr. R. A. Jacobson and his gorup for continuing X-ray crystallographic services and to Dr. S. D. Wijeyesekera for help in obtaining and interpreting the extended Hückel results.

Supplementary Material Available: Tabulations of the anisotropic temperature factors and the observed and calculated structure factors for the four structures studied and the atomic coordinates and orbital parameters used in the extended Hückel calculations (13 pages). Ordering information is given on any current masthead page.

(38) Kematick, R. J.; Franzen, H. F.; Misemer, D. K. *J. Solid State Chem.* **1985**, *60*, 297.
(39) Ziebarth, R. P.; Corbett, J. D., to be published.
(40) Hwu, S.-J.; Corbett, J. D. *J. Solid State Chem.*, submitted for publication.
(41) Schwanitz-Schüller, U.; Simon, A. *Z. Naturforsch. B* **1985**, *40*, 705.
(42) Warkentin, E.; Simon, A. *Rev. Chim. Miner.* **1983**, *20*, 488.
(43) Heaton, B. T. In "Organometallic Chemistry"; Royal Society of Chemistry: London, 1983; Vol. 12 p 143.
(44) Soloveichik, G. L.; Bulychev, B. M.; Semenenko, K. N. *Russ. J. Coord. Chem.* **1983**, *9*, 891.
(45) Raithby, P. R. In "Transition Metal Clusters"; Johnson, B. F. G., Ed.; John Wiley and Sons: Chichester, UK, 1980; p 9.
(46) Corbett, J. D.; Daake, R. L.; Poeppelmeier, K. R.; Guthrie, D. H. *J. Am. Chem. Soc.* **1978**, *100*, 652.